Effective and lesion-free cutaneous influenza vaccination

Ji Wang[1], Bo Li[1], and Mei X. Wu[2]

Wellman Center for Photomedicine, Massachusetts General Hospital, and Department of Dermatology, Harvard Medical School, Boston, MA 02114

Edited by Philippa Marrack, Howard Hughes Medical Institute, National Jewish Health, Denver, CO, and approved March 10, 2015 (received for review January 8, 2015)

The current study details efficient lesion-free cutaneous vaccination via vaccine delivery into an array of micropores in the skin, instead of bolus injection at a single site. Such delivery effectively segregated vaccine-induced inflammation, resulting in rapid resolution of the inflammation, provided that distances between any two micropores were sufficient. When the inoculation site was treated by FDA-approved nonablative fractional laser (NAFL) before insertion of a PR8 model influenza vaccine-packaged, biodegradable microneedle array (MNs), mice displayed vigorous antigen-uptake, eliciting strong Th1-biased immunity. These animals were completely protected from homologous viral challenges, and fully or partially protected from heterologous H1N1 and H3N2 viral challenges, whereas mice receiving MNs alone suffered from severe illnesses or died of similar viral challenges. NAFL-mediated adjuvanicity was ascribed primarily to dsDNA and other "danger" signals released from laser-damaged skin cells. Thus, mice deficient in dsDNA-sensing pathway, but not Toll like receptor (TLR) or inflammasome pathways, showed poor responses to NAFL. Importantly, with this novel approach both mice and swine exhibited strong protective immunity without incurring any appreciable skin irritation, in sharp contrast to the overt skin irritation caused by intradermal injections. The effective lesion-free cutaneous vaccination merits further clinical studies.

biodegradable microneedle | nonablative fractional laser | dsDNA

Substantial evidence has shown that skin is a more potent site for vaccination than muscle because the former contains a large number of antigen presenting cells (APCs) and abundant network of lymphatic vessels. Moreover, skin offers potential for painless, needle-free, and self-applicable immunization, which would particularly benefit annual influenza vaccination of large populations (1, 2). However, skin immunization has not been broadly adopted to date, due to lack of safe adjuvants and technical difficulties in injecting vaccines into the ultrathin (<2 mm) skin tissue (3, 4). We have demonstrated that controllable skin injury can serve as safe "adjuvant" for cutaneous vaccination and similar observations have been also made by other investigators (5–7). Treatment of the inoculation site with nonablative fractional laser (NAFL) generates an array of microthermal zones (MTZs) beneath the stratum corneum (8). The dying cells in the MTZs release "danger" signals that provoke sterile inflammation that is however constrained within individual MTZs. This array of microsterile inflammatory zones is resolved quickly, effectively averting skin lesion, provided that affected and unaffected areas of the skin are adequately balanced (8). Importantly, despite fast resolution, the microinflammation zones prove sufficient in augmentation of adaptive immune responses against the vaccine (5). In addition, this standalone adjuvant does not affect the volume of administration or formulation of the vaccine, which are serious hurdles for skin immunization because only a limited volume and nonviscous vaccines are suitable for skin injection (9). In this regard, emulsion-based adjuvants like Alum and MF59 are excluded from a use as cutaneous adjuvant owing to strong and persistent skin reactions induced by the adjuvants (3, 4, 10).

Apart from adjuvants, intradermal (ID) delivery of influenza vaccine not only is challenging but also provokes a high rate of pain and skin irritation compared with intramuscular (IM) immunization. In the last decade, a variety of strategies have been explored to deliver vaccines into the skin, among which microneedle has received considerable attentions (11). The technology uses single or an array of ultra-short and ultra-thin needles to penetrate into the skin for vaccine delivery. These microneedles are long enough to cross the stratum corneum barrier, but short enough to avoid pain, offering a method for minimally invasive and painless vaccine delivery. Notably, an intradermal microinjection system has already been approved for delivering a reduced dose (9 μg) of seasonal influenza vaccine in adults in USA and Europe and a typical dose (15 μg) in the elderly in Europe. The thinner and shorter microneedle (1.5 mm in length) reduces pain significantly. The pain may be further reduced by a microneedle array (MNs) or a patch where each array contains hundreds or thousands of tiny microneedles (12–15). To load a sufficient amount of vaccine in a patch, these microneedles are usually densely packed in a small patch (~1 cm^2). Nevertheless, these highly dense microneedle arrays hardly address skin reactogenicity in relevant animal models.

To robustly reduce or completely eliminate skin lesion, we expanded the microfractional concept from adjuvant to vaccine delivery in the current study. We fabricated an array of biodegradable microneedles with sufficient distances between individual microneedles to constrain vaccine-induced inflammation. Prevention of vaccine-induced inflammation from spreading into nearby micropores warranted rapid resolution of inflammation as well as minimal skin lesion. Moreover, when influenza

Significance

Skin is more potent than muscle for vaccination, but it is not yet a common site for immunization, in part owing to relatively high rates of pain and skin irritation and difficulty of administration. We resolve this dilemma by delivering vaccines into many micropores in the skin, which constrains vaccine-induced inflammation, leading to fast healing and lesion-free. Moreover, combination of microfractional vaccine delivery with nonablative fractional laser (NAFL), not only significantly augmented vaccine efficiency but also broadened cross-protection against homologous and heterologous influenza viral infections. Cross-protective immunity is pivotal for influenza vaccines because mismatches occur frequently between vaccine viral strains and circulating viruses. To the best of our knowledge, this represents the first strategy for lesion-free efficient cutaneous vaccination.

Author contributions: M.X.W. designed research; J.W. and B.L. performed research; J.W., B.L., and M.X.W. analyzed data; and J.W. and M.X.W. wrote the paper.

The authors declare no conflict of interest.

This article is a PNAS Direct Submission.

[1]J.W. and B.L. contributed equally to this work.

[2]To whom correspondence should be addressed. Email: mwu5@mgh.harvard.edu.

This article contains supporting information online at www.pnas.org/lookup/suppl/doi:10.1073/pnas.1500408112/-/DCSupplemental.

vaccine-packaged MNs was applied into a NAFL-treated site, the vaccine induced much broader immunity against homo- and heterologous strains of influenza viruses than the array alone in mice. The combination also gave rise to strong protective immunity but with little skin lesion in swine, an animal model with skin resembling that of humans.

Results

Optimization of Microneedle Density. Arrays of 6 × 9 microneedles at varying densities were fabricated using biodegradable polyvinylpyrrolidone (PVP) as described (14, 16). One of the arrays was held by two fingers and a part of the array was shown in Fig. 1*A*. A tip-to-tip distance of 4 bases is illustrated in Fig. 1*B*, *Upper*, where one base refers to the base diameter of a microneedle. A representative fluorescent image of three microneedles coated with fluorescent sulphorhodamine B (SRB) in the array was given in Fig. 1*B*, *Upper*. The microneedles were degraded within 15 min after insertion into the porcine skin ex vivo (Fig. 1*B*, *Lower*). *Bacillus* Calmette–Guérin vaccine was mixed with PVP to generate bacillus Calmette–Guérin–MNs to address a relationship between microneedle density and local skin reactions. Bacillus Calmette–Guérin is an FDA approved, intradermal vaccine and it causes severe local reactions in humans and mice (9, 17, 18). The array was applied into the skin of C57BL/6 mice for 15 min, and skin reactions were analyzed 48 h later. In parallel, the same amount of bacillus Calmette–Guérin prepared from one bacillus Calmette–Guérin–MNs was ID administered by a hypodermal needle as controls. ID vaccination caused obvious skin irritation, manifesting a wheal 0.3–0.5 cm in diameter, erythema, and swelling (Fig. 1*C*). The skin reactogenicity occurred soon after immunization, peaked for 2–5 d, and was not resolved in 12 d. The skin irritation was alleviated, but penetrated into a relatively big area while a 2× base bacillus Calmette–Guérin–MNs was applied into the skin (Fig. 1*C*). The skin reactions were still seen with a 3× or 4× base bacillus Calmette–Guérin–MNs, albeit at a much lesser degree than those attained with the 2× base array. When the distance between two microneedles increased to 5× bases, skin reaction was hardly seen at the inoculation site (Fig. 1*C*).

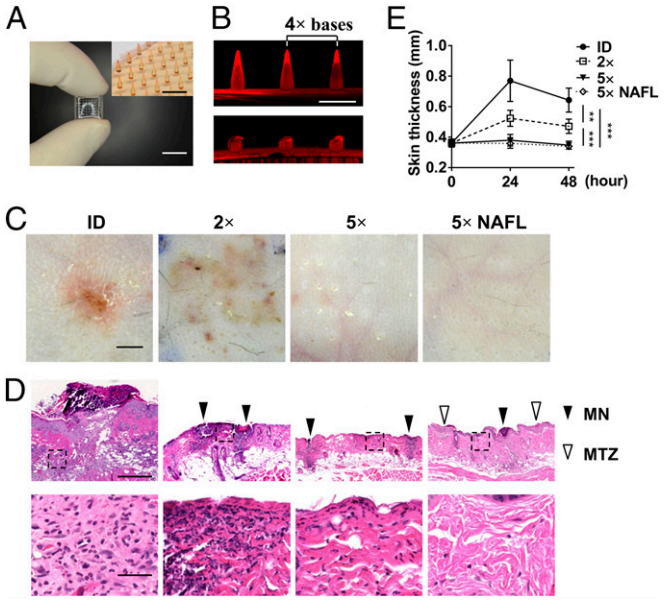

Fig. 1. Effects of microneedle density on skin inflammation. (*A*) MNs. A microneedle array is held by two fingers. (*Inset*) A portion of SRB-loaded MNs. (Scale bar, 1 cm or 1 mm in *Inset*.) (*B*) Three representative microneedles in the array before insertion (*Upper*) and after insertion (*Lower*). A tip-to-tip distance of 4× bases is indicated in the upper panel. (Scale bar, 600 μm.) (*C*) Skin reaction in the inoculation sites. bacillus Calmette–Guérin vaccine was administered into mice either by intradermal injection (ID) or MNs at a tip-to-tip distance of 2× base diameters (2×) or 5× base diameters (5×). A 5× bacillus Calmette–Guérin-MNs was also applied into the skin after NAFL treatment. Photos were taken 48 h after immunization. (Scale bar, 2 mm.) (*D*) H&E stained slides of corresponding inoculation sites. Solid triangles indicate microneedle injection sites, opened triangles point MTZs induced by NAFL, and an area outlined by a dashed square in upper panel was enlarged in the corresponding lower panel. (Scale bar, 400 μm in *Upper* and 50 μm in *Lower*.) (*E*) Skin thicknesses measured at different time points after immunization. $n = 8$. $^{**}P < 0.01$, $^{***}P < 0.001$. Each photo in *A*–*D* represents four similar results.

Histological examination revealed that ID injection of bacillus Calmette–Guérin vaccine induced severe inflammations and heavy infiltrates of inflammatory cells at the inoculation site (Fig. 1*D*, first column), concurrent with skin thickening (Fig. 1*E*). In contrast, microfractional delivery of the same amount of bacillus Calmette–Guérin by MNs induced milder inflammation (Fig. 1*D*, second column). Although the skin became thicker after immunization, the degree of such thickening was much lesser in mice receiving a 2× base bacillus Calmette–Guérin–MNs compared with mice receiving ID injection (Fig. 1*E*). Further lowering the microneedle density by increasing a tip-to-tip distance to 5× bases almost completely averted skin reactions as measured by both skin inflammation and thickness (Fig. 1*D*, third column, and Fig. 1*E*). Notably, inflammation induced by individual microneedles spread into the neighbor microzones with a 2× base bacillus Calmette–Guérin–MNs (Fig. 1*D*, second column), whereas the inflammation in each microzone was well segregated in a 5× base bacillus Calmette–Guérin–MNs without any overlap (Fig. 1*D*, third column). The observations corroborate that constraining inflammation within individual microzones is pivotal for lesion-free vaccination. The 5× base MNs was chosen for subsequent vaccinations.

Lowering microneedle density, although vigorously diminishing skin reactions, substantially reduces the vaccine loading capacity of the array, which is problematic as a large area of the skin may be required to deliver a vaccine. This dilemma can be circumvented by a standalone laser vaccine adjuvant that boosts immune responses, leading to significant dose-sparing, as we previously demonstrated (5). We confirmed that NAFL did not affect skin inflammation or thickness compared with the array alone control (Fig. 1 *C*–*E*).

NAFL Enhances Antigen-Uptake by APCs Inside and Outside MTZs Similarly. Our previous investigation showed that laser treatment augmented antigen uptake (19, 20). It was not known, however, whether the antigen should be delivered directly into NAFL-induced MTZs, because APCs activated by NAFL accumulated around each MTZ (Fig. 2*A*) (5). Alternatively, antigen deposition in areas near MTZs might allow equivalent antigen capture. To determine this, we first illuminated the inoculation site with NAFL creating a 6 × 9 array of MTZs, followed by 15-min application of MNs with the same 6 × 9 pattern in a manner either precisely matching or mismatching between MTZs and MNs as depicted in Fig. S1*B*, first column. The array was fabricated with AlexaFlour-647–labeled ovalbumin (OVA-AF647) that permitted tracking an uptake of the delivered antigen. As shown in Fig. S1*A*, highly concentrated OVA labeled by red fluorescence was distributed in the same pattern as the MNs in the skin, suggesting a sufficient delivery. The OVA-AF647 signal could be detected as deep as 200 μm by two-photon confocal microscopy and a representative image of OVA delivered by one microneedle was shown in Fig. S1*A*. In the absence of NAFL, the majority (80%) of OVA-AF647 remained in the skin 1 d after MNs application, and ~40% of OVA was still detectable in 3 d (Fig. S1 *B* and *C*). In sharp contrast, a much weaker and scattered distribution of OVA was observed 1 d following MNs application, and only 15% of

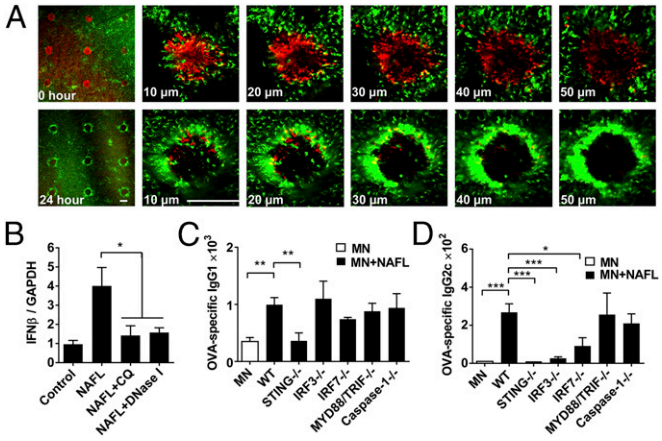

Fig. 2. dsDNA released from dying cells mediates adjuvant effect of NAFL. (*A*) An MTZ array generated by NAFL showing dsDNA (red) staining. Intensive dsDNA staining was seen immediately after laser treatment, but disappeared in 24 h (first column). Different layers of an enlarged MTZ were scanned (right columns) and the number in each panel indicates the depth of the MTZ relative to the skin surface. (Scale bar, 200 μm.) (*B*) C57BL/6 mice were treated with NAFL alone, NAFL plus chloroquine (CQ), or NAFL plus DNase I. Dermal IFNβ mRNA levels were measured by real-time qPCR. $n = 4$. Wild-type mice (WT) or indicated knockout (–/–) mice were immunized with OVA-MNs in the presence or absence of NAFL. Serum IgG1 (*C*) and IgG2c (*D*) antibody titers were measured 2 wk later by ELISA. $n = 6$. $^{*}P < 0.05$, $^{**}P < 0.01$, $^{***}P < 0.001$. All experiments were repeated twice with similar results.

OVA could be detected in 3 d when mice received NAFL before application of MNs (Fig. S1 *B* and *C*). Unexpectedly, NAFL treatment greatly accelerated the uptake and transportation of antigens regardless of whether the MNs was precisely matched or mismatched with the array of MTZs (Fig. S1*B*). Perhaps soluble mediators like chemokines, cytokines induced by laser-damaged cells were essential in mobilization of APCs toward antigens in the vicinity (5). The finding greatly simplified the technology because matching MTZs and MNs would not only make it difficult to apply the MNs, but also limit the type of MNs used. The diminished amount of antigen seen in the skin was inversely correlated with an increasing number of antigen-loaded APCs identified as OVA^{+}APCs in the draining lymph nodes one day after the immunization ($P < 0.05$, Fig. S1*D*). Once again, there was no significant difference in the number of OVA^{+}APCs in the draining lymph nodes regardless of whether the MNs was mismatched or matched with MTZs. As expected, MNs in conjunction with NAFL induced OVA-specific IgG production at a level significantly higher than that induced by MNs alone, irrespective of whether the antigen was delivered inside or outside MTZs ($P < 0.01$, Fig. S1*E*). In conclusion, NAFL treatment of the inoculation site can enhance the uptake and transportation of antigens delivered presumably by any MNs, augmenting the efficiency of vaccines.

Adjuvant Effect of NAFL Is Mediated by dsDNA. We previously showed that laser-damaged cells inside MTZs were responsible for the adjuvant effect (5). Some "danger" signals released from the damaged cells appeared to endure at high temperatures, indicating that nucleic acids released from dead cells might be involved. To corroborate this, we first developed a new method to track the double strand DNA (dsDNA) released from dead cells in live animals. A cell impermeable dsDNA dye DRAQ7 was s.c. injected beneath the site of NAFL-treated skin. We used s.c. rather than intradermal injection to avoid additional skin injuries at the laser-treated site warranting a clear background. Within 15–30 min of injection, DRAQ7 penetrated into the dermis and then epidermis, and stained dsDNA that was released from or inside dying cells. The staining was clearly seen from less than 10 μm up to more than 50 μm from skin surface in or around each MTZ (Fig. 2*A*). The dsDNA staining was robust immediately after NAFL treatment, but mostly disappeared one day later, concurrent with heavy accumulations of APCs around individual MTZs (Fig. 2*A*). The APCs expressed GFP-conjugated MHC-II molecule and were comprised of dendritic cells (DCs), Langerhans cells, and macrophages. Disappearance of dsDNA might be attributed to their uptake by APCs, degradation or both, but not to a loss of DRAQ7 dye, because the weak staining could not be reversed if additional DRAQ7 was administered in the second day.

We next addressed a role for NAFL-induced dsDNA release in its adjuvant effect. We observed a significant increase in the transcription of IFN beta (IFN-β), a marker of dsDNA sensing pathway, at the NAFL-treated site. The increase in IFN-β transcription was blunted by chloroquine (CQ), which abrogates the uptake of dsDNA by endocytosis (21), or DNase I that digests dsDNA directly (22), confirming dsDNA's direct involvement in IFN-β induction (Fig. 2*B*). A further study with mice deficient in a specific innate immune pathway revealed that TLR (MyD88/$TRIF^{-/-}$) and inflammasome (Caspase-$1^{-/-}$) pathways had little impact on NAFL-mediated enhancement of Th1 (IgG2c) or Th2 (IgG1) responses (Fig. 2 *C* and *D*). On the contrary, deficiency in the stimulator of IFN gene (STING) significantly impaired both responses with a more prominent effect on Th1 immunity (Fig. 2 *C* and *D*), in good agreement with a key adaptor of STING in dsDNA sensing pathway (23). The finding that interferons (IFNs) were indispensable for NAFL-mediated enhancement of Th1 immune response was also corroborated by a blunted IgG2c response in mice lacking either IFN regulatory factor (IRF) 3 or, to a lesser degree, IRF7 (Fig. 2*D*). Unlike Th1 immunity, IFNs were dispensable for Th2 immune response, as suggested by unaltered IgG1 production in mice lacking either IRF3 or IRF7 (Fig. 2*C*). An involvement of STING but not IRF3 or IRF7 argues that Th2 immune responses enhanced by the dsDNA pathway may result from other cytokines (Fig. 2*C*).

Enhancement of Influenza Vaccines by Using MNs at the NAFL-Treated Site. We went on to test how NAFL affected the immune response elicited by influenza vaccine delivered by MNs. To this end, the lower dorsal skin of mice was illuminated by NAFL, followed by insertion of MNs containing 0.4 μg of hemaglutinin (HA) equivalent H1N1 PR8 model influenza vaccine. The array was also dissolved in 20 μL PBS for ID or IM injection by a hypodermic needle as controls. The mean HAI titers of ID and MNs alone were similar at 1:53, more than twofold better than those attained with IM vaccination (1: 20). NAFL treatment raised the HAI titer by more than 5 times, to 1:278, compared with MNs alone (Fig. 3*A*). Interestingly, NAFL elevated HAI titers at levels significantly higher when the vaccine was administered by MNs than ID ($P < 0.01$, Fig. 3*A*). NAFL treatment, in combination with MNs, not only raised HAI titers, but also augmented a Th1-biased immune response (Fig. 3*B*). The combined approach had much less influence over Th2 immune responses (Fig. 3*C*). Opposing adjuvant effects of NAFL were seen after ID vaccination, with a more predominant effect on Th2 immune responses reflected by higher IgG1 levels, concomitant with lower IgG2a production compared with MNs+NAFL immunization (Fig. 3 *B* and *C*). Consequently, NAFL treatment of the site of MNs insertion profoundly raised IgG2a/IgG1 ratios compared with all other immunizations tested (Fig. 3*D*). These results stress that MNs in place of ID delivery not only augments the vaccination but also converts the immune response into a more protective one by NAFL, all while producing no lesion or pain.

Apart from humoral immune responses, NAFL treatment also greatly augmented cellular immune responses irrespective of

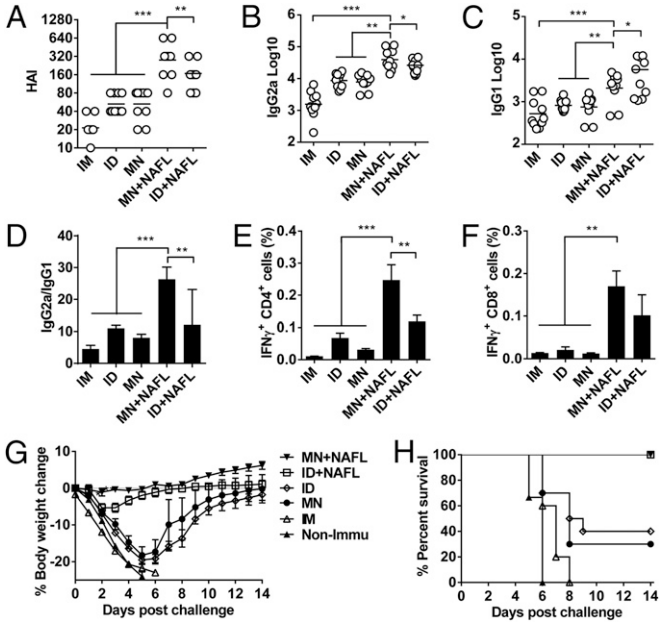

Fig. 3. NAFL augments protective immunity elicited by influenza vaccine-MNs. Swiss Webster mice were immunized with influenza vaccine (PR8 strain, 0.4 μg HA) by ID or MNs in the presence or absence of NAFL. IM immunization was carried out for comparison. Four weeks after immunization, serum HAI (*A*), IgG2a (*B*), or IgG1 (*C*) titers were measured by ELISA. IgG2a/IgG1 ratios are shown in *D*. $n = 10$. Cellular immune responses were measured one week after the immunization. Peripheral blood mononuclear cells were stimulated by inactivated influenza virus, and percentages of IFNγ secreting $CD4^+$ (*E*) or $CD8^+$ (*F*) were measured by flow cytometry. $n = 10$. Mice were challenged with influenza virus (PR8 strain, 5,000× LD_{50}) 5 wk after immunization. Body weight changes and survival rates were shown in *G* and *H*, respectively. $n = 10$. $^*P < 0.05$, $^{**}P < 0.01$, and $^{***}P < 0.001$. All experiments were repeated twice with similar results.

whether the vaccine was administered by MNs or ID. As can be seen in Fig. 3 *E* and *F*, $CD4^+$ T cells secreting IFN-γ were significantly higher in MNs+NAFL group ($P < 0.01$), whereas $CD8^+$ T cells secreting IFN-γ were vigorously elevated in both ID and MNs groups following NAFL.

NAFL Significantly Broadens Immunity Induced by Influenza Vaccine-Packaged MNs. Influenza viral strains used in the preparation of seasonal influenza vaccines often slightly mismatch the circulating viruses due to constant gene mutations of the virus, reducing the efficacy of the vaccines. To test whether NAFL plus MNs could elicit a broadened immunity against homologous as well as heterologous viral strains, we first challenged mice with 5×10^3 LD_{50} PR8 H1N1 influenza virus 5 wk after immunization with PR8 viral vaccine. This high dose viral challenge killed all nonimmunized mice within 6 d with a body weight loss >25% (Fig. 3 *G* and *H*). IM immunization did not protect any of the animals either. ID or MNs immunization provided only limited protection with a similar survival rate <50% (4 of 10 and 3 of 10, respectively). Strikingly, all mice survived the viral challenge when they received NAFL treatment before MNs application or ID immunization (10 of 10, Fig. 3*H*). The vigorous immune protection was also strongly indicated by no body weight loss at all in the MNs+NAFL group or only less than 5% body weight loss on day 3 after viral infection in ID+NAFL group (Fig. 3*G*).

Apparently, a combination of NAFL and MNs delivery was a better strategy to augment immune responses against influenza viral infection. Thus, this strategy was tested for cross-protection against heterologous viral strains. Accordingly, mice were immunized with PR8 H1N1 vaccine-packaged MNs in the presence or absence of NAFL as above and challenged in 2 wk with 10× LD_{50} of two H1N1 viruses, A/California/7/2009 or A/New Caledonia/20/1999, or one H3N2 (A/Aichi/2/1968) influenza virus. As shown in Fig. 4, PR8 H1N1 vaccination conferred a high level of cross-protection against A/California/7/2009 (100%) and A/New Caledonia/20/1999 (>80%) H1N1 viruses (Fig. 4 *A* and *C*), or modest protection against a genetically distant H3N2 virus (50%) (Fig. 4*E*) in the presence of NAFL, although the mice experienced moderate to severe body weight losses (Fig. 4 *B*, *D*, and *F*). In marked contrast, little or no protection was seen in mice receiving the same influenza vaccine in the absence of NAFL, as measured by both survival rates and body weight loses (Fig. 4). Conceivably, incorporation of NAFL into influenza vaccination could greatly enhance the efficacy of the vaccines even with mismatched viral strains circulating in the flu season.

Validation of Effective and Lesion-Free Vaccination in Swine. Swine is frequently used to evaluate both the efficacy and skin reactogenicity of cutaneous vaccination because of a similarity between human and porcine skins. Yorkshire pigs at 4 mo of age were thus immunized by ID, MNs, MNs+NAFL delivery of PR8 influenza vaccine (Fig. 5*A*). Two MNs carrying a total of 2 μg of HA protein were used for the immunization of each pig at contralateral sites in the presence or absence of NAFL. ID immunization was performed by hypodermal needle injection of 100 μL of vaccine prepared from one array and each pig received two injections of the same amount of PR8 vaccine at corresponding sites. ID injection of PR8 influenza vaccine induced significant erythema and wheal at injection sites, which were persistent for at least 5 d (Fig. 5*A*, first panel). The severe local reactions could not be ascribed to poor quality of the vaccine, because ID injection of clinical seasonal influenza vaccine induced comparable local reactions (Fig. 5*A*, fourth panel), as has been well documented in humans (24, 25). In sharp contrast, there were no visible erythema, wheal or other skin reactions occurring at the inoculation site after 15 min of vaccination with MNs in the presence (Fig. 5*A*, third panel) or absence (Fig. 5*A*, second panel) of NAFL treatment, although NAFL did induce slight redness that quickly disappeared within 30 min (Fig. 5*A*, third panel). Confirmation of a lesion-free process in the swine model is highly clinically relevant.

Apparently, lesion-free delivery with MNs did not compromise immunity induced by the vaccine compared with ID (Fig. 5*B*), despite lack of overt skin inflammation, consistent with previous investigations showing that prolonged inflammation at the

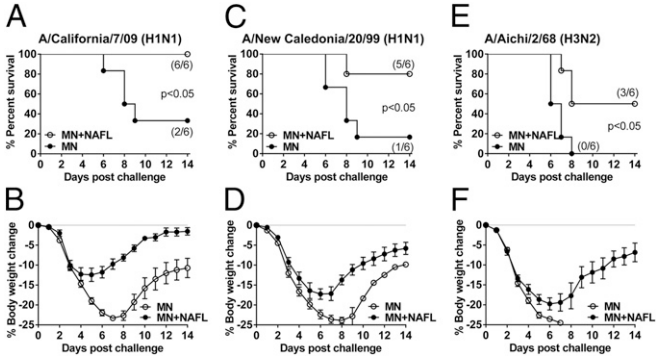

Fig. 4. NAFL broadens cross-protective immunity against influenza virus. Swiss Webster mice were immunized with influenza vaccine (PR8 strain, 0.4 μg of HA) by MNs alone or in the presence of NAFL. Two weeks after immunization, mice were challenged with indicated heterologous strains of influenza viruses at a dose of 10× LD_{50} per mouse. Survival rates (*A*, *C*, and *E*) and body weight changes (*B*, *D*, and *F*) were monitored for 14 d. $n = 6$. All experiments were repeated twice with similar results.

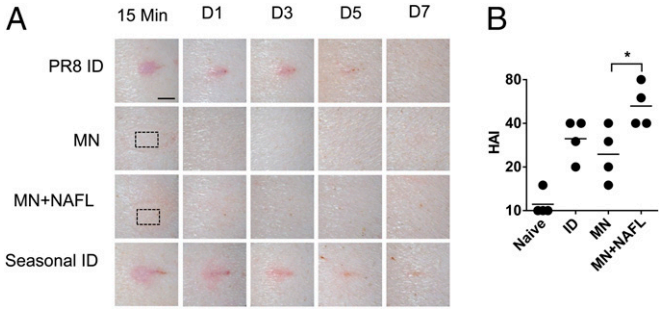

Fig. 5. Validation of effective, lesion-free vaccination in swine . (*A*) Yorkshire pigs were immunized with influenza vaccine (PR8) by ID, MNs alone, or MNs following NAFL treatment. Seasonal influenza vaccine (2013–2014 formulation) was ID administered as skin reaction control. Photos were taken at indicated times after immunization. Each photo represents four similar results. The dashed rectangle indicates the MNs application site. (Scale bar, 5 mm.) (*B*) HAI titers were measured 2 wk after immunization. $*P < 0.05$.

inoculation site was not necessary for effective immunization (5, 26). Moreover, in comparison with vaccination of MNs alone, NAFL treatment significantly enhanced the immune responses, without incurring any adverse events. These results suggest that effective, lesion-free cutaneous vaccination could be achieved by a combination of MNs and NAFL.

Discussion

Biodegradable MNs take advantages of the skin not only as a more potent immunization site, but also as a potentially painless, needle-free, and self-applicable vaccination site. The current investigation suggests that a density of MNs is crucial for lesion-free delivery, an issue that has not been well addressed so far, to the best of our knowledge. Loading a high amount of vaccines into biodegradable MNs is always an issue, because a majority of the microneedle shaft must be filled with polymerization matrix to ensure the mechanical strength of the microneedle (27). Unfortunately, this limitation cannot be resolved by increasing a length of the microneedles because long microneedles cause pain (28). Our present study showed that a 2× base bacillus Calmette–Guérin–MNs provoked severe skin irritation. The high density of microneedle arrays may also diminish the penetration capability (29, 30). It was found that >5× base MNs provided the best penetration capability in human skin (29, 30). This, along with our finding that a 5× base MNs offers lesion-free delivery, argues strongly that 5× base MNs would be ideal for vaccine delivery, but such less dense MNs would further limit the loading capacity of biodegradable MNs. This dilemma can be effectively addressed by employment of NAFL as shown in our study. Pretreatment of the inoculation site with NAFL augmented the efficacy of MNs-delivered influenza vaccine by at least fourfold (Fig. 3*A*) and thus reduced the patch size by ∼75%.

NAFL not only resolves the dilemma between the vaccine loading capacity and an optimal density of MNs, but also significantly broadens the immunity of influenza vaccines. Immunization with MNs in the presence of NAFL completely protected mice from homologous (PR8 H1N1) viral challenge at a high dose, exhibiting no body weight loss and a 100% survival rate, whereas immunization with MNs alone gave poor protection as suggested by a severe body weight loss and only a 30% survival rate. Additionally, the immunization conferred a broader spectrum of cross-protection against other H1N1 influenza viruses and a totally different subtype H3N2 influenza virus. Cross-protective immunity is extremely important for seasonal influenza vaccines because a mismatch in vaccine viral strains and circulating viral strains occurs frequently, reducing the efficacy of seasonal influenza vaccines substantially. Such a mismatch took place in 2009 when a new H1N1 influenza viral strain emerged, to which seasonal flu vaccines offered little protection, resulting in a higher morbidity rate in the population <65 y of age (31). In the flu season 2012–2013, a mismatch was also reported for H3N2 virus and the efficacy of the seasonal influenza vaccines was only ∼50% in adults or 9% in the elderly in that year, which was apparently too low to be accepted (32). Early data suggested that roughly half of the H3N2 virus were mismatched with the vaccine H3N2 viral strain in this flu season (2014–2015). These unpredictable mutations highlight necessity of eliciting cross-protective immunity against influenza viruses. Conceivably, cross-protection even within the same viral subtype may substantially reduce the mortality and morbidity induced by mismatched influenza viruses. The standalone NAFL adjuvant can be applied on an as-needed basis, for instance, if viral strains of seasonal influenza vaccines differ from circulating influenza viruses in the flu season. Although a whole inactivated viral vaccine was used in the study, similar immune enhancement of NAFL was attained with the licensed split or HA subunit influenza vaccines ID administered (5). Whether NAFL can also augment the cross protection elicited by MNs packaged with split or subunit flu vaccines is under current investigation.

In an attempt to comprehend how NAFL could vigorously augment immunity in the absence of overt skin inflammation, mice deficient in individual major innate immune pathways, including TLRs, dsDNA, and inflammasome, were tested. Our results clearly showed that the dsDNA-sensing pathway, but not TLRs or inflammasome pathways, participated in augmentation of the immune responses by NAFL. Following NAFL-mediated microtissue damage, dsDNA is released from dying cells, taken up by APCs, or transported into cytosol, presumably with assistance of antimicrobial peptides that are also highly expressed during skin tissue damage (33, 34). dsDNA, a damage-associated molecule, binds to a number of dsDNA sensors (23). Upon binding to the sensor, the activation signal is transduced to the adaptor protein STING (35), followed by activation of Type I IFN transcription through a TBK1-IRF3–mediated pathway or by activation of proinflammatory cytokines through NFκB pathway (36). Activation of cGAS-STING sensing pathway was recently found to be important for IFN induction (37, 38) and likely one of the major players in NAFL-mediated adjvuanicity, as suggested by a high level of IFN-β transcription following NAFL treatment and abolishment of the production by DNase I or chloroquine (Fig. 2*B*). Although STING was critical for both Th1 and Th2 immune responses, the IRF3-IRF7 pathway might be responsible only for Th1 immune responses (Fig. 2 *C* and *D*). The result indicates that other proinflammatory cytokines may be involved in NAFL-mediated Th2 immune responses. dsDNA released from dying host cells appears to have a universal role for various adjuvants. For example, the commonly used alum adjuvant is found to be toxic to cells, killing host cells and causing dsDNA release (22, 39). Sensing of dsDNA may be a key to the immunogenicity of DNA vaccine as well. In support, B and T-cell–mediated immune responses induced by DNA vaccine were greatly impaired in STING-deficient mice (35). Moreover, the transfer of tumor-derived dsDNA and subsequent activation of STING-IRF3 pathway have been shown to sufficiently augment $CD8^+$ T-cell responses against tumor cells (40). Because dsDNA not only takes central part in adjuvant effects, but also participates in other processes including wound healing (41), psoriasis (21), systemic lupus erythematosus (42), etc., we developed a novel method to in vivo track dsDNA release in skin, which may be useful in tracking dsDNA release in the skin in a variety of conditions.

Intriguingly, a Th1 immune response is predominant when NAFL is paired with MNs, whereas a Th2 immune response is biased if NAFL is combined with ID delivery (Fig. 3). The difference may not result from the amount of dsDNA release as

NAFL treatment of the inoculation site similarly, and rather, a prolonged inflammation induced by ID injection may tilt toward a Th2-biased immune response. It is well known that skin injury is healed by expansion of surrounding healthy epithelial cells to close the injury. The larger the skin-injured area is, the longer the closure takes. On the other hand, if many micropores are generated in the skin with a total injured area equivalent to one injury, these well separated micropores would heal much quicker than would such an injury, because it takes only a day or two for each micropore to be fully closed, but weeks for the injury to be healed (15). This repair capacity forms the basis of cosmetic skin resurfacing in dermatology, where laser or MNs are used to make these micropores. The quick healing may be essential not only for lesion-free vaccination, but also for Th1-baised immunity. After skin injury, a Th1 immune response is prominent at the early phase of skin repair, which is followed by a Th2-skewed immune response in the late phase of the repair (43). Constraining inflammation within individual micropores results in resolution of the inflammation fast enough to avoid the late Th2-biased immune response. This observation reinforces that a short period of local sterile inflammation is enough to "educate" DCs in bridging an innate to adaptive immune response as we previously demonstrated (5). This important notion is strongly supported by the investigation showing that surgical removal of the inoculation site containing alum 2 h after vaccination did not compromise the adjuvant effect of alum (26). The study, along with our observations, argues strongly the dispensability of prolonged inflammation at the inoculation site for effective vaccination. Hence, extending the microfractional concept to vaccine/adjuvant delivery not only minimizes skin lesion or inflammation, but also enhances protective Th1-predominant immunity.

The current study demonstrates efficient and lesion-free cutaneous vaccination by combining MNs and NAFL to fractionally deliver vaccines/adjuvant into dozens of micropores in the skin. Microfractional delivery vigorously reduces skin lesion and inflammation but increases immune responses provoked by the vaccine with a Th1-predominant, broader immune response. The effective and safe strategy warrants clinical studies immediately. In the future, NAFL and application of MNs can be engineered into a single, small handheld device and used repeatedly for influenza vaccination in a cost-effective manner.

Materials and Methods

An FDA-approved nonablative fractional laser, PaloVia, was used in mice (PaloVia, Palomar Medical Technologies). Pigs were treated with Fraxel SR-1500 laser (Solta Medical). Microneedle arrays were prepared as described (14, 16). Data are presented as mean ± SEM; *P* value was calculated by PRISM software (GraphPad) and a difference was regarded significant if *P* value was less than 0.05. Full details of methods are described in *SI Materials and Methods*.

ACKNOWLEDGMENTS. We thank Photopathology Core for their help in the histology and flow cytometry analysis during this project and Jeffrey H. Wu for editing. This work is supported in part by the National Institutes of Health Grants AI089779, AI070785, AI097696, and DA028378 (to M.X.W.).

1. Karande P, Mitragotri S (2010) Transcutaneous immunization: An overview of advantages, disease targets, vaccines, and delivery technologies. *Annu Rev Chem Biomol Eng* 1:175–201.
2. Kim YC, Prausnitz MR (2011) Enabling skin vaccination using new delivery technologies. *Drug Deliv Transl Res* 1(1):7–12.
3. Chen X, Wu MX (2011) Laser vaccine adjuvant for cutaneous immunization. *Expert Rev Vaccines* 10(10):1397–1403.
4. Chen X, Pravetoni M, Bhayana B, Pentel PR, Wu MX (2012) High immunogenicity of nicotine vaccines obtained by intradermal delivery with safe adjuvants. *Vaccine* 31(1): 159–164.
5. Wang J, Shah D, Chen X, Anderson RR, Wu MX (2014) A micro-sterile inflammation array as an adjuvant for influenza vaccines. *Nat Commun* 5:4447.
6. Depelsenaire AC, et al. (2014) Colocalization of cell death with antigen deposition in skin enhances vaccine immunogenicity. *J Invest Dermatol* 134(9):2361–2370.
7. Chen X, Wang J, Shah D, Wu MX (2013) An update on the use of laser technology in skin vaccination. *Expert Rev Vaccines* 12(11):1313–1323.
8. Manstein D, Herron GS, Sink RK, Tanner H, Anderson RR (2004) Fractional photothermolysis: A new concept for cutaneous remodeling using microscopic patterns of thermal injury. *Lasers Surg Med* 34(5):426–438.
9. Zehrung D, Jarrahian C, Wales A (2013) Intradermal delivery for vaccine dose sparing: overview of current issues. *Vaccine* 31(34):3392–3395.
10. Hickling JK, et al. (2011) Intradermal delivery of vaccines: potential benefits and current challenges. *Bull World Health Organ* 89(3):221–226.
11. Hickling J, Jones R, PATH, World Health Organization (2009) *Intradermal Delivery of Vaccines: A Review of the Literature and the Potential for Development for use in Low- and Middle-Income Countries* (PATH, Seattle).
12. Prow TW, et al. (2010) Nanopatch-targeted skin vaccination against West Nile Virus and Chikungunya virus in mice. *Small* 6(16):1776–1784.
13. Bachy V, et al. (2013) Langerin negative dendritic cells promote potent CD8+ T-cell priming by skin delivery of live adenovirus vaccine microneedle arrays. *Proc Natl Acad Sci USA* 110(8):3041–3046.
14. Sullivan SP, et al. (2010) Dissolving polymer microneedle patches for influenza vaccination. *Nat Med* 16(8):915–920.
15. Kim YC, Park JH, Prausnitz MR (2012) Microneedles for drug and vaccine delivery. *Adv Drug Deliv Rev* 64(14):1547–1568.
16. Yang SY, et al. (2013) A bio-inspired swellable microneedle adhesive for mechanical interlocking with tissue. *Nat Commun* 4:1702.
17. Trinchieri G, Sher A (2007) Cooperation of Toll-like receptor signals in innate immune defence. *Nat Rev Immunol* 7(3):179–190.
18. Chen X, Kositratna G, Zhou C, Manstein D, Wu MX (2014) Micro-fractional epidermal powder delivery for improved skin vaccination. *J Control Release* 192:310–316.
19. Chen X, et al. (2010) A novel laser vaccine adjuvant increases the motility of antigen presenting cells. *PLoS ONE* 5(10):e13776.
20. Chen X, et al. (2012) Facilitation of transcutaneous drug delivery and vaccine immunization by a safe laser technology. *J Control Release* 159(1):43–51.
21. Lande R, et al. (2007) Plasmacytoid dendritic cells sense self-DNA coupled with antimicrobial peptide. *Nature* 449(7162):564–569.
22. Marichal T, et al. (2011) DNA released from dying host cells mediates aluminum adjuvant activity. *Nat Med* 17(8):996–1002.
23. Wu J, Chen ZJ (2014) Innate immune sensing and signaling of cytosolic nucleic acids. *Annu Rev Immunol* 32:461–488.
24. Beran J, et al. (2009) Intradermal influenza vaccination of healthy adults using a new microinjection system: A 3-year randomised controlled safety and immunogenicity trial. *BMC Med* 7:13-7015-7-13.
25. Leroux-Roels I, et al. (2008) Seasonal influenza vaccine delivered by intradermal microinjection: A randomised controlled safety and immunogenicity trial in adults. *Vaccine* 26(51):6614–6619.
26. Hutchison S, et al. (2012) Antigen depot is not required for alum adjuvanticity. *FASEB J* 26(3):1272–1279.
27. Vrdoljak A (2013) Review of recent literature on microneedle vaccine delivery technologies. *Vaccine Dev Therapy* 3:47–55.
28. Gill HS, Denson DD, Burris BA, Prausnitz MR (2008) Effect of microneedle design on pain in human volunteers. *Clin J Pain* 24(7):585–594.
29. Kochhar JS, et al. (2013) Effect of microneedle geometry and supporting substrate on microneedle array penetration into skin. *J Pharm Sci* 102(11):4100–4108.
30. Yan G, Warner KS, Zhang J, Sharma S, Gale BK (2010) Evaluation needle length and density of microneedle arrays in the pretreatment of skin for transdermal drug delivery. *Int J Pharm* 391(1-2):7–12.
31. Hancock K, et al. (2009) Cross-reactive antibody responses to the 2009 pandemic H1N1 influenza virus. *N Engl J Med* 361(20):1945–1952.
32. Skowronski DM, et al. (2014) Low 2012-13 influenza vaccine effectiveness associated with mutation in the egg-adapted H3N2 vaccine strain not antigenic drift in circulating viruses. *PLoS ONE* 9(3):e92153.
33. Chamilos G, et al. (2012) Cytosolic sensing of extracellular self-DNA transported into monocytes by the antimicrobial peptide LL37. *Blood* 120(18):3699–3707.
34. Sørensen OE, et al. (2003) Wound healing and expression of antimicrobial peptides/polypeptides in human keratinocytes, a consequence of common growth factors. *J Immunol* 170(11):5583–5589.
35. Ishikawa H, Ma Z, Barber GN (2009) STING regulates intracellular DNA-mediated, type I interferon-dependent innate immunity. *Nature* 461(7265):788–792.
36. Paludan SR, Bowie AG (2013) Immune sensing of DNA. *Immunity* 38(5):870–880.
37. Wu J, et al. (2013) Cyclic GMP-AMP is an endogenous second messenger in innate immune signaling by cytosolic DNA. *Science* 339(6121):826–830.
38. Sun L, Wu J, Du F, Chen X, Chen ZJ (2013) Cyclic GMP-AMP synthase is a cytosolic DNA sensor that activates the type I interferon pathway. *Science* 339(6121):786–791.
39. McKee AS, et al. (2013) Host DNA released in response to aluminum adjuvant enhances MHC class II-mediated antigen presentation and prolongs CD4 T-cell interactions with dendritic cells. *Proc Natl Acad Sci USA* 110(12):E1122–E1131.
40. Woo SR, et al. (2014) STING-dependent cytosolic DNA sensing mediates innate immune recognition of immunogenic tumors. *Immunity* 41(5):830–842.
41. Gregorio J, et al. (2010) Plasmacytoid dendritic cells sense skin injury and promote wound healing through type I interferons. *J Exp Med* 207(13):2921–2930.
42. Lande R, et al. (2011) Neutrophils activate plasmacytoid dendritic cells by releasing self-DNA-peptide complexes in systemic lupus erythematosus. *Sci Transl Med* 3(73): 73ra19.
43. Rani M, Zhang Q, Schwacha MG (2014) Burn wound γδ T-cells support a Th2 and Th17 immune response. *J Burn Care Res* 35(1):46–53.